Available online at www.sciencedirect.com
ScienceDirect
International Journal of Rock Mechanics & Mining Sciences 45 (2008) 609–620
International Journal of Rock Mechanics and Mining Sciences
www.elsevier.com/locate/ijrmms

Technical Note

Multivariate statistical techniques for evaluating the effects of brecciated rock fabric on ultrasonic wave propagation

Javier Martínez-Martínez[a,b,*], David Benavente[a,b], Salvador Ordóñez[a,b], M. Ángeles García-del-Cura[b,c]

[a]*Departamento de Ciencias de la Tierra y del Medio Ambiente, Universidad de Alicante, Ap. 99, 03080 Alicante, Spain*
[b]*Laboratorio de Petrología Aplicada, Unidad Asociada CSIC-UA, Alicante, Spain*
[c]*Instituto de Geología Económica, CSIC-UCM, Madrid, Spain*

Received 24 November 2006; received in revised form 28 June 2007; accepted 18 July 2007
Available online 24 September 2007

1. Introduction

The texture and structure of rocks are important parameters for characterizing rock types from a petrophysical and mechanical point of view. The shape and size of the mineral grains, the existence of preferred orientation in fractures, or the matrix content, for example, are some of the most important parameters which control the response of materials in petrophysical tests [1–7].

Two of the most important problems when studying the influence of rock fabric in the petrophysical behaviour of materials are the correct quantification of petrographic characters of rocks, and the handling of the analysis of multivariables with correlations. Several techniques and methods have been developed in order to solve the first problem [4,6,8–11], whilst the second question is not usually dealt with in depth.

Many studies use bivariate analysis in order to assess the influence of both textural and petrophysical parameters [10,12–14]. However, it is often not possible to reduce the study of the influence of texture in a physical process to a two-variable problem due to the fact that different petrographic parameters are usually dependant on each other so that it is hard to separate them as independent variables. Therefore, to merely analyse the interrelation between two parameters is not sufficient to understand the physical behaviour of a rock in most cases.

In this paper, an in-depth study of the correlation between petrographic features and ultrasonic waves is carried out. The ultrasonic method is an extremely useful, non-destructive test for evaluating the mechanical properties of rocks [15–24]. This method is based on the propagation of high-frequency elastic waves through materials. In contrast with destructive tests, the analysis of the propagation of ultrasonic waves through materials allows an estimate of the mechanical properties of rocks to be obtained without destroying the sample used. This is an important advantage as it may be applied simultaneously with different tests as well as measurements can be repeated on the same sample. The propagation of ultrasonic waves through materials is strongly and simultaneously influenced by different petrographic aspects (fractures, porosity, crystal-size, preferred orientations, etc.). Consequently, a bivariate analysis of these influences is not particularly useful.

For multivariate analysis, our rock samples were characterized in terms of several petrographic parameters obtained by means of colour image analysis. Image analysis is a field that is rapidly expanding due to advances in modern computer technology, which award to this method easy accessibility, low cost and consistently accurate results. In this study, a new method has been designed in order to quantify petrographic characteristics by means of colour image analysis processing [25], given that the complex characteristics of the highly fractured materials and the conditions of this study mean that methods published in previous literature cannot be applied [1,10,26,27]. The numerically quantified outcomes are composed of several petrographic variables, for example,

*Corresponding author. Departamento de Ciencias de la Tierra y del Medio Ambiente, Universidad de Alicante, Ap. 99, 03080 Alicante, Spain. Tel./fax: +34 965 903727.
E-mail address: javier.martinez@ua.es (J. Martínez-Martínez).

1365-1609/$ - see front matter
doi:10.1016/j.ijrmms.2007.07.021

fine-grained matrix content, brecciation density (*bd*) or preferred clasts orientations. These numeric parameters are essential if a multivariate analysis is to be carried out.

Secondly, several ultrasonic parameters have been calculated from the digital analysis of the transmitted signals in order to obtain as numerical ultrasonic information as possible. In this study, four ultrasonic parameters have been calculated: compressional and shear wave velocities (V_p and V_s, respectively), velocity ratio (V_p/V_s) and waveform energy (ε). Moreover, the dynamic elastic constants, Young's modulus (E_d) and Poisson's ratio (v_d), have been calculated from ultrasonic velocities and bulk density in order to assess the mechanical characteristics of the rocks.

The aim of this paper is to analyse the interaction between the petrographic parameters and ultrasonic characters in highly fractured materials. This analysis has been carried out by applying different multivariate analysis tools: scatter diagrams, principal components and cluster analysis. The results obtained allow for an in-depth understanding of the interrelation between rock fabric and the ultrasonic test, which is extremely useful in assessing the degree of fracturing of rocks, the preferred orientation of the fracture sets, elastic constants, and, in short, the mechanical quality of rocks.

2. Materials

Two different varieties of brecciated dolostone have been used in this study: Marrón Emperador (ME) and Beige Serpiente (BS). These kinds of rocks are widely used as a construction and building material, mainly for cladding, flooring and paving. The mechanical behaviour of these brecciated dolostones plays an essential role in such uses, in ensuring the correct use and high durability of these materials.

2.1. Marrón Emperador

Marrón Emperador (ME) is defined as a highly fractured dolostone (Fig. 1). In this variety, abundant fractures with strong dissolution processes are observed, although no preferred orientation has been noted. This fractured system defines clasts that vary greatly in size. In general, texture of clasts corresponds to microcrystalline and/or mesocrystalline dolostones (according to Friedman's terminology, 1965). The cement, which surrounds the clasts and fills the veins, is over 90% calcite (Fig. 1c). Total porosity of the sample varies between 2.6% and 4.2%, depending on the degree of fracturing (according to [28]).

2.2. Beige Serpiente

Beige Serpiente (BS) corresponds to a breccia where clasts are not clearly defined by fractures (Fig. 1). In this case, as in the ME variety, texture of clasts corresponds to microcrystalline and/or mesocrystalline dolostones, although limestone fragments are not often present. Clast size distribution is more homogeneous than in the previous case, even though small clasts are more abundant. Many clasts show thin white calcite veins which have a low continuity. The fine-grained matrix, which surrounds the clasts, is formed by a mixture of calcite (20%) and dolomite (80%) crystals. The porosity associated to the fine-grained matrix is relatively high (approximately 8.5%, according to [28]) and millimetric-size geodes can sometimes develop.

3. Methodology

3.1. Image analysis

In this study, four cubic samples ($7 \times 7 \times 7$ cm) of each variety were used. This geometry allows three orthogonal axis systems to be defined and used as reference system.

The petrographic features of the samples used have been quantified by means of colour image analysis. Several software packages have been used in order to obtain good rock fabric quantification. It was necessary to design a specific methodology due to the great complexity of the chromatic characteristics, the heterogeneity of these rocks, and the need to carry out a mesoscopic study [25].

The image was obtained by scanning the moistened surfaces of the samples (Fig. 2a). This procedure was chosen as it offers both the best lighting conditions and a good resolution for the subsequent image analysis. A mesoscale study was required, rather than the more common microscopic analysis, as the average size of the elements studied (clasts, veins, etc.) was in the order of a few centimetres.

Several filters were applied to remove isolated erroneous pixels from the image obtained (noise reduction): *Median filter* and *lowpass filter*. The aim of this step is to improve the quality of the image as well as to provide a more effective segmentation of the image.

Image segmentation consists of identifying and defining the clasts of the materials. The result of this step is an image in which clasts and fine-grained matrix are completely differentiated. In order to carry out this differentiation, two processes are distinguished: *Primary* and *secondary segmentation*. Primary segmentation (Fig. 2b) is an automatic process where a rough differentiation is obtained. This step is carried out via the manual threshold method. This method are carried out selecting the whole pixels included between two threshold values previously defined, and encoding them with the same colour, and different from the remainder pixels. The upper and lower thresholds in our images are established taking into account the particular histogram of each clast (Fig. 2). In this way, the global thresholds include the mean chromatic range of clasts. These values are necessarily defined again when a new image is analysed due to the high chromatic heterogeneity of materials (especially in BS variety). The image obtained after this step shows clasts not completely isolated due to some erroneous pixels of fine-grained matrix, which have similar chromatic

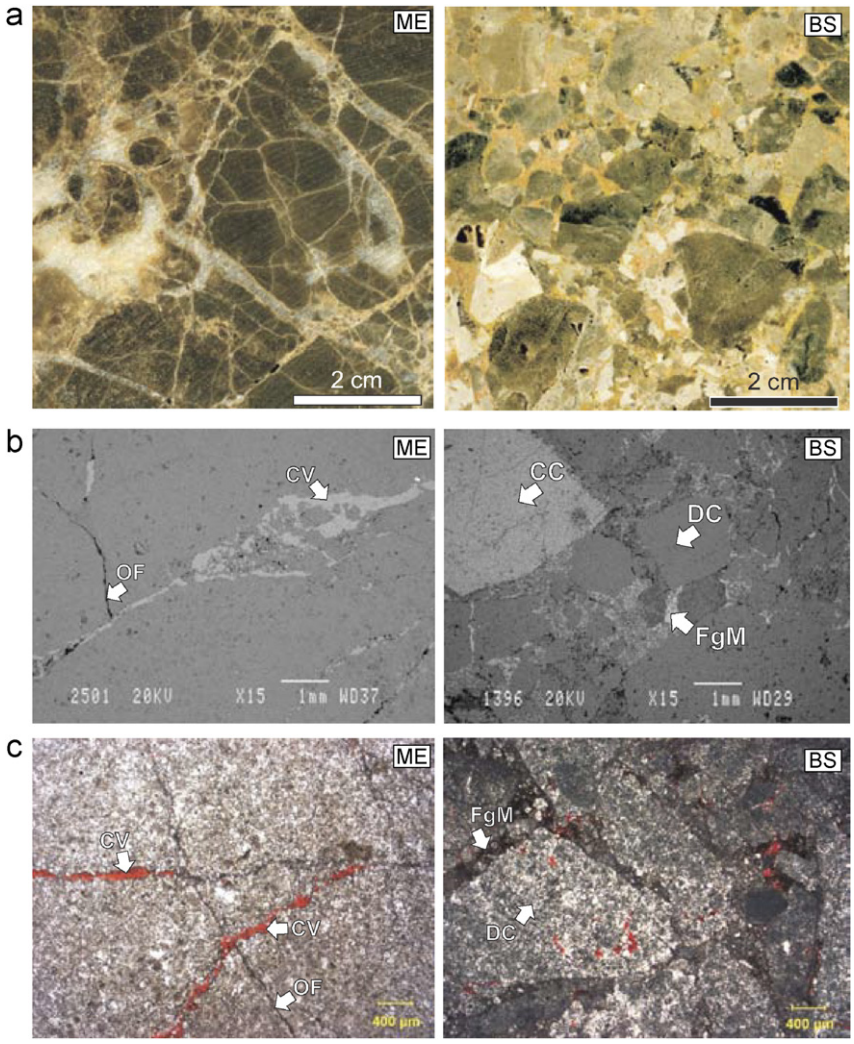

Fig. 1. The two studied varieties (Marrón Emperador: ME; Beige Serpiente: BS) as observed (a) at mesoscale; (b) under scanning electron microscope in backscattering secondary electron mode (SEM-BSE); and (c) under optical polarising microscope (the sample was stained with Alizarin Red S). CV: calcite vein; OF: open fracture; CC: calcite clast; DC: dolomite clast; FgM: fine-grained matrix.

coordinates to clasts. The secondary segmentation (Fig. 2c) is a manual process where these erroneous pixels are removed, and the clasts are completely isolated from the fine-grained matrix.

The result of this step is a binary image (Fig. 2c) in which the original image has been reduced to a two-colour scheme: the black areas correspond to clasts and the white areas correspond to the fine-grained matrix. From binary images several parameters can be calculated, which have been designed in order to quantify specific rock fabric characteristics of materials. These parameters are:

Brecciation density (*bd*): This parameter is obtained in order to quantify the brecciation degree of the rock sample. Brecciation density is defined as the number of clasts content per surface unit. When a net, whose cells measure $1\,cm^2$, is placed over the image, *bd* is defined as the percentage of cells with a content equal to or more than six clasts. The counting of the number of clasts per surface unit is carried out with Maltlab® v.5.3, and consists in comparing the coordinates of the net nodes and the coordinates of the centroids of the clasts [25]. In this way, a high value in the *bd* parameter corresponds to a high small clast content. Therefore, the sample is associated to a strong brecciation process.

Clast size distribution: The clasts have been classified according to their area in six size classes (Table 1). The different classes express the number of clasts whose area is included within the thresholds of that class.

Fine-grained matrix content in the sample (*FMC*): As a result of the segmentation process, the code of the binary image corresponds white pixels to the fine-grained matrix and black pixels to clasts. This fact allows us to quantify the fine-grained matrix content by calculating the percentage of pixels, which were codified in white in the binary image. This is a very important parameter in the analysis of the relationship between rock fabric and ultrasonic waves. This importance lies in the fact that fine-grained matrix is formed on average by 90% of calcite in ME and 20% in

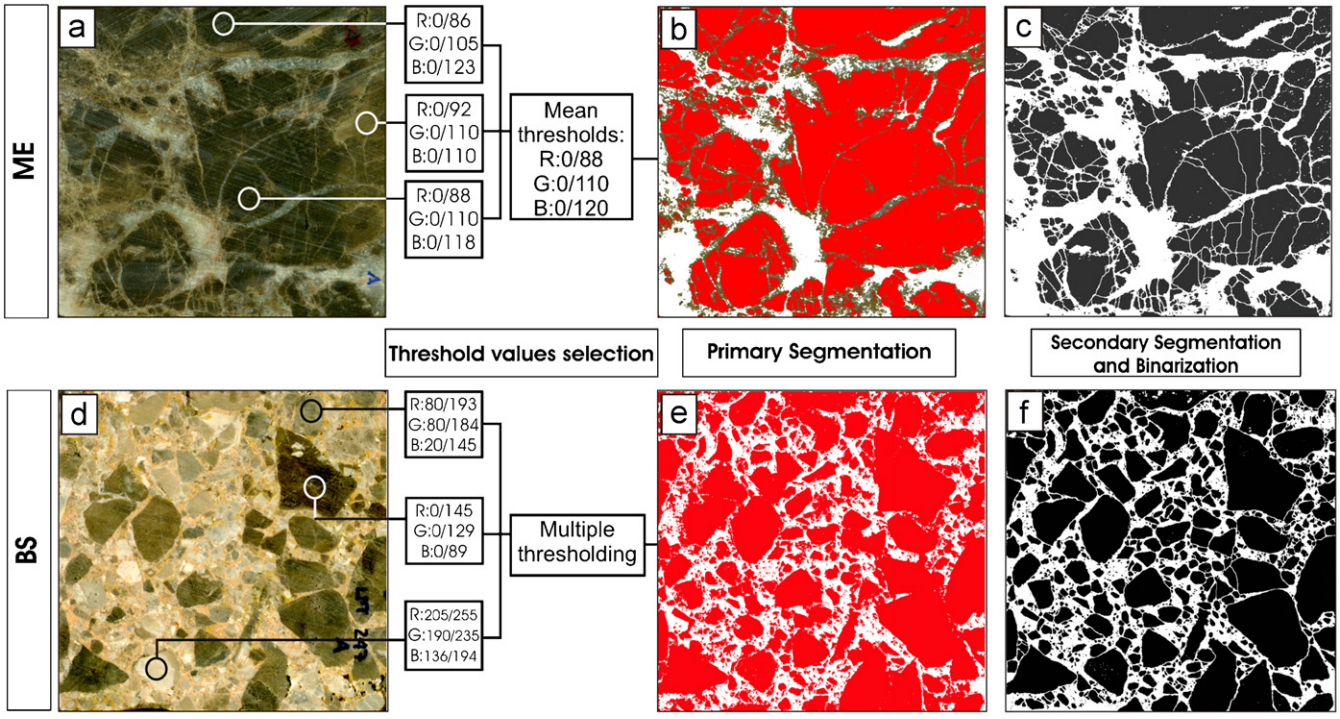

Fig. 2. Image analysis process used to quantify the most important petrographic features of the samples studied. Images (a), (b) and (c) correspond to Marrón Emperador (ME) variety, whereas images (d), (e) and (f) correspond to a Beige Serpiente (BS) sample. Images (a) and (d): scanned sample surface; images (b) and (e): primary segmentation; images (c) and (f): secondary segmentation and final binary image. The step between images (a) and (b) as well as between (d) and (e) shows the thresholds selection process.

Table 1
Size class limits

Class	Class1	Class2	Class3	Class4	Class5	Class6
Scale of values (cm^2)	<0.03	0.03–0.44	0.44–0.84	0.84–1.24	1.24–1.64	>1.64

BS. Therefore, FMC is an indirect measurement of the calcite content in the sample. Different FMC values can be translated into different calcite/dolomite ratios, and consequently, different associated ultrasonic velocities.

Preferred clast orientations (α_{lim}): The importance of the presence of clast preferred orientations is based on the fact that this clast preferred orientation can be extrapolated to discontinuity orientations. This extrapolation can occur when only elongated clasts are considered. Consequently, this analysis has been realised taking only into account the clasts whose minor axis length to major axis length ratio is less than 0.6. In these particles, the orientation of boundaries, or the fractures, which define boundaries, can be considered the same as the major axis angle of the clast (Fig. 3).

Due to the need to effectively quantify the discontinuity orientations, the parameter α_{lim} is defined as the percentage of elongated clasts orientated in the least favourable direction as regards ultrasonic wave propagation (Fig. 4). In order to obtain the worst orientation of clasts for ultrasound, a theoretical critical angle has been obtained. According to the wave theory, when a wave strikes a discontinuity, there exist specific angles between the wave direction and the discontinuity surface in which refracted waves are not generated. Elongated clasts with a major axis angle included in these orientations are the particles with the least favourable conditions for wave propagation. This assertion is due to the fact that the boundaries of elongated clasts are sub-parallel to their major axis and therefore, these discontinuities cause a total wave reflection.

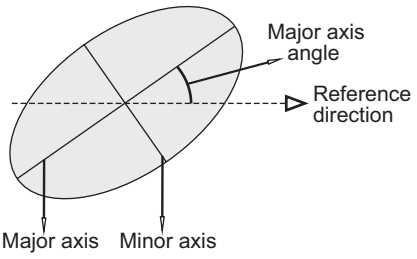

Fig. 3. Diagram of a hypothetical clast, showing its major and minor axes and its major axis angle.

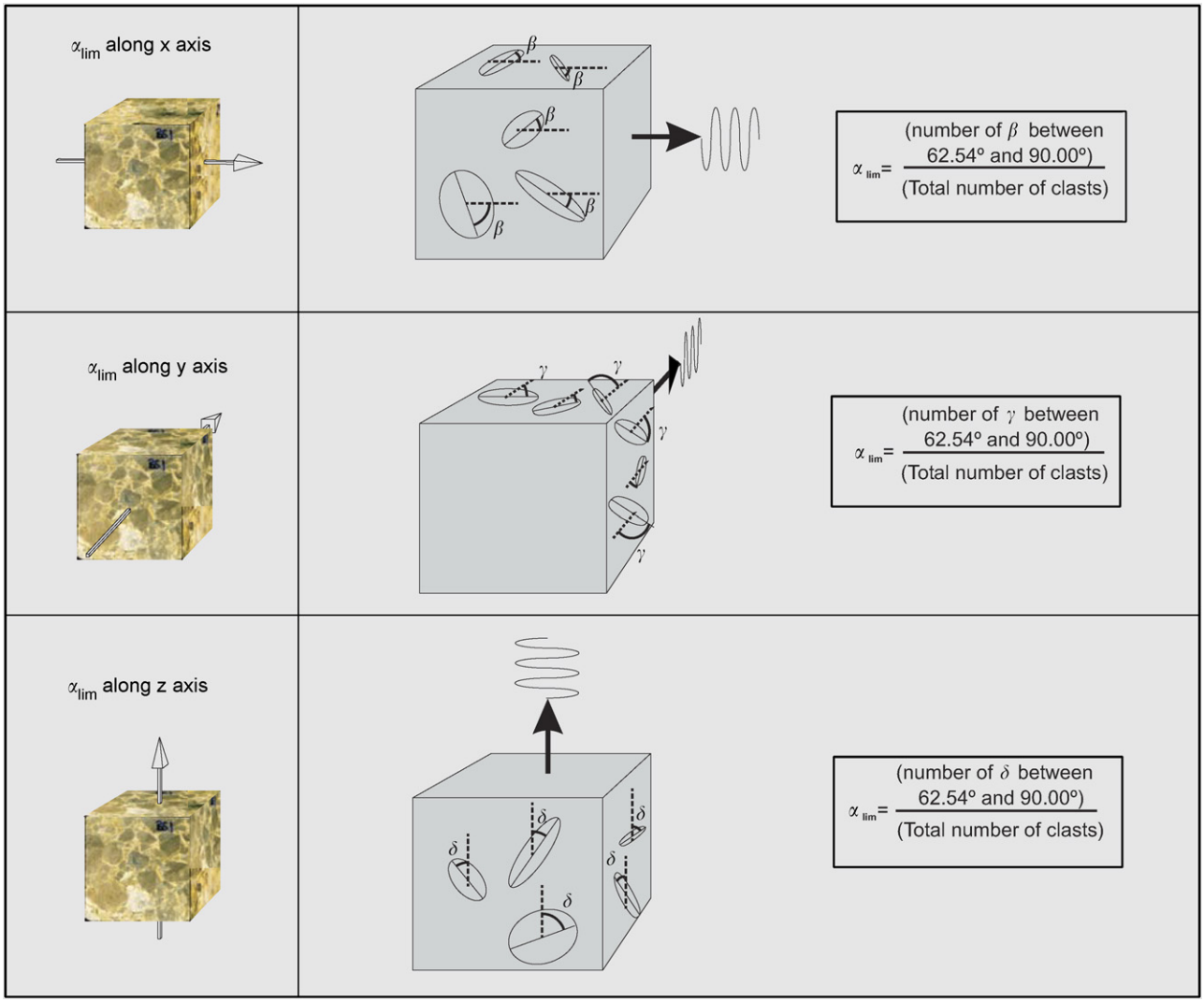

Fig. 4. Diagram of the calculation of the α_{lim} after the three orthogonal axes defined in the sample. The parameter α_{lim} in each direction is calculated as the ratio between (1) the number of elongated clasts orientated in the least favourable direction as regards ultrasonic wave propagation, counted in the four parallel surfaces to the direction in which the ultrasonic wave was measured and (2) the total number of clasts in the four parallel surfaces to the direction of the ultrasonic measurement.

This critical angle for a wave that strikes a boundary between a calcitic medium and a dolomitic medium, the only case where refraction is produced, is 62.54°, according to Snell's law [29,30]. Therefore, the parameter α_{lim} quantifies the percentage of clasts which fulfill both conditions, which is on the one hand, their elongation is equal to or less than 0.60 and, on the other, their major axis angle is between $\pm 62.54^{\circ}$ and $\pm 90.00^{\circ}$.

The parameter α_{lim} is calculated on each surface of the sample (six values per cubic sample). In order to obtain a comparable single value of the ultrasonic parameters, the mean of the four parallel surfaces to the direction in which the ultrasonic wave was measured has been calculated. In short, α_{lim} is the global percentage of clasts, and discontinuities, which are orientated in the least favourable direction as regards ultrasonic wave propagation.

When the value of a specific parameter depends on the direction considered in the sample, three different values are calculated in each direction of its orthogonal axis systems. The specific conditions of this methodology are indicated in [25].

3.2. Ultrasonic measurements

In order to obtain reproducible conditions in the ultrasonic measurement, the samples were dried at 60 °C for 48 h. After they had been cooled in a desiccator, each one was weighed in order to obtain the bulk density.

The ultrasonic transmission method was used. This involves two piezoelectric sensors coupled to the object at constant pressure by means of the hand procedure. One of the transducers is stimulated using an ultrasonic pulser and the other is used as a receptor sensor. Therefore, this method measures the propagation wave characteristics induced by microstructural factors. Compressional (P) and shear (S) waves were measured using polarised Panametric

transducers (500 kHz) and a Sonic Viewer-170, which acquired and digitalised waveforms to be displayed, manipulated and stored. A visco-elastic couplant was used to achieve good coupling between the transducer and the sample.

Several ultrasonic parameters have been calculated from the digital analysis of the transmitted signal. The most widely used ultrasonic parameter in material strength determination is compressional wave velocity, V_p. However, the analysis of the elastic wave propagation can be substantially enhanced when digital analysis of the ultrasonic signal is used [20,21]. In this study, several ultrasonic parameters have been calculated. However, four of them have been selected as the most interesting: compressional and shear wave velocities (V_p and V_s, respectively), velocity ratio (V_p/V_s) and waveform energy (ε). All of these ultrasonic parameters were determined from the mean of a minimum of three measurements for each direction considered.

Propagation velocity (both V_p and V_s) was determined from the ratio of the length of the specimen to the transit time of the pulse. Waveform energy (ε) is presented in a dimensionless form and is defined as the integral of the area under the square rectified amplitude.

Young's dynamic modulus of elasticity (E_d) and Poisson's ratio (v) were calculated from *P*-wave and *S*-wave velocities (Eqs. (1) and (2)) in order to assess the elastic behaviour of the rocks [31]:

$$E = \rho_{bulk} V_p^2 \frac{(1-2v)(1+v)}{(1-v)}, \quad (1)$$

$$v = \frac{(V_p/V_s)^2 - 2}{2[(V_p/V_s)^2 - 1]}. \quad (2)$$

3.3. Multivariate analysis

Three different multivariate analysis statistical tools were applied for stabilising the structure of the variable dependence and the interrelationship. The strategy employed in the statistical analysis is summarised in the following steps: (1) a principal component analysis (PCA), which was applied to the database in order to obtain correlations between the different parameters calculated; (2) a scatter diagram analysis, which allows a particular bivariate study of the correlations observed in the PCA; (3) a cluster analysis, to analyse the overall similar characteristics patterns of the two previously described materials.

3.3.1. Principal component analysis

The principal component analysis involves a mathematical procedure that transforms a number of correlated variables into a smaller number of uncorrelated variables called *principal components*. Each component is a weighted, linear combination of the original variables. Usually, only components with an eigenvalue greater than 1 are of any interest. In order to make the components more interpretable, while still being orthogonal, a varimax rotation is used.

3.3.2. Scatter diagrams

Scatter diagrams are a kind of illustration, which allow a different distribution of the variables' data (normal or log-normal) to be recognised and the correlation level between two parameters to be analysed.

3.3.3. Cluster analysis

Cluster analysis is a popular technique used to find groups of data [32]. In clustering, the objects are grouped into clusters so that the degree of association is strong between members of the same cluster and weak between members of different clusters. Objects in one cluster should be homogeneous, with respect to certain characteristics describing properties, and well separated from elements in other clusters. This separation of clusters is based on multivariate distance.

4. Results and discussion

Ultrasonic parameters (compressional and shear wave velocities, velocity ratio and waveform energy), and dynamic elasticity constants are shown in Table 2. The average value of: brecciation density (*bd*), preferred clasts orientation (α_{lim}), fine-grained matrix content (FMC) and density are shown in Table 3. The size-class distribution of clasts are shown in Table 4.

4.1. Principal component analysis and scatter diagrams

The principal component analysis was carried out using the code SPSS v.11.5.1 (from SPSS Inc.). The ultrasonic parameters considered in this analysis are V_p, V_s and V_p/V_s. The log(ε) values were also included due to the fact that ε reveals a logarithmic distribution regarding both ultrasonic and petrographic parameters.

Six petrographic parameters were selected: *bd*, α_{lim}, FMC, density, Class2 and Class5. Only two classes (Class2 and Class5) have been chosen to carry out the current multivariate analysis due to the fact that only Class1, Class2 and Class5 present significant different clast content between BS and ME varieties. Class3, Class4 and Class6 present similar content in both materials and do not contribute to differentiate the ultrasonic response between both varieties. On the other hand, the size range of the clasts contained in Class1 is small comparing to the ultrasonic wave sensitivity. According to previous statements, Class2 represents the lowest size class whose clasts are recognised by the propagated ultrasonic wave (as the size of these clasts is greater than the wave sensitivity threshold). On the other hand, Class5 represents the highest size class in which there are enough differences between the varieties studied. Both dynamic elastic

Table 2
Values of both ultrasonic parameters and dynamic elasticity constants

		V_p (m/s)	V_s (m/s)	V_p/V_s	log(ε)	$Ed \times 10^2$ (GPa)	v_d
ME-I	x	5820	2700	2.15	10.71	8.50	0.36
	y	5140	2280	2.27	10.52	3.70	0.38
	z	5190	2730	1.89	10.21	5.20	0.30
ME-II	x	6210	3280	1.91	12.48	7.50	0.31
	y	5920	3160	1.91	11.92	6.80	0.31
	z	6460	3190	1.98	12.34	7.60	0.33
ME-III	x	5220	2860	1.99	11.65	5.00	0.33
	y	5390	2910	1.98	11.92	5.30	0.33
	z	5000	2730	1.94	11.53	4.70	0.32
ME-IV	x	5230	2930	1.91	11.75	5.30	0.31
	y	5390	2960	1.96	11.88	5.40	0.33
	z	5300	2910	1.92	11.56	5.40	0.31
BS-I	x	5070	2920	1.76	12.58	5.60	0.26
	y	5010	2900	1.74	12.47	5.50	0.25
	z	5300	2940	1.87	12.74	5.50	0.30
BS-II	x	6140	3730	1.67	12.93	8.90	0.22
	y	6420	3440	1.80	12.70	8.70	0.28
	z	5990	3260	1.84	12.12	7.30	0.29
BS-III	x	5600	3010	1.83	12.80	6.40	0.29
	y	5410	2960	1.79	12.81	6.20	0.27
	z	5600	2980	1.90	12.74	6.00	0.31
BS-IV	x	6440	3320	1.94	12.68	7.80	0.32
	y	6240	3310	1.87	12.47	7.80	0.30
	z	5980	3250	1.84	13.04	7.30	0.29

ME: Marrón Emperador variety; BS: Beige Serpiente variety.

Table 3
Values of: *bd*, α_{lim}, FMC and density, of both Marrón Emperador and Beige Serpiente varieties (ME and BS, respectively)

		bd (%)	α_{lim} (%)	FMC (%)	Density (g/cm^3)
ME-I	x	49.52	22.36	4.77	2.65
	y		34.21		
	z		24.57		
ME-II	x	46.59	25.8	5.98	2.69
	y		30.05		
	z		20.56		
ME-III	x	59.15	32.45	27.73	2.7
	y		33.2		
	z		24.95		
ME-IV	x	56.8	32.39	29.68	2.69
	y		30.61		
	z		25.96		
BS-I	x	75.17	24.66	6.14	2.65
	y		23.76		
	z		20.85		
BS-II	x	66.66	19.53	5.42	2.67
	y		25.01		
	z		24.15		
BS-III	x	79.58	24.81	6.71	2.65
	y		23.38		
	z		19.65		
BS-IV	x	48.97	23.46	3.67	2.68
	y		25.94		
	z		19.29		

constants, Young's modulus and Poisson's ratio, have been considered in this analysis.

Four principal components were extracted which accounted for 90.8% of the total variance, using Varimax as a factor rotation method. The coefficients of the different variables in these four components are shown in Table 5. There are two remarkable aspects in these coefficients: (1) the absolute value of coefficients: high values in several coefficients of the same component reveal a narrow relationship between them; (2) the sign of the coefficient: the same or opposite sign of several coefficients reveal the direct or inverse relationship between them.

Table 4
Size-class distribution of clasts

Size-class distribution (%)	Class1	Class2	Class3	Class4	Class5	Class6
ME-I	209	120	6	3	1	1
ME-II	201	113	8	2	1	4
ME-III	242	127	6	1	1	1
ME-IV	222	120	7	2	1	3
BS-I	354	126	68	5	83	3
BS-II	427	99	6	2	1	3
BS-III	388	132	81	3	60	2
BS-IV	348	73	79	1	65	2

ME: Marrón Emperador variety; BS: Beige Serpiente variety.

Table 5
Coefficients of the different variables in the four components obtained by principal component analysis

	Component			
	1	2	3	4
% explained of the total variance	28.412	23.641	22.510	16.311
bd	−0.475	−0.259	0.772	−0.111
α_{lim}	0.018	0.076	−0.758	0.463
FMC	−0.470	0.142	−0.173	0.815
Class2	−0.885	−0.066	0.049	0.055
Class5	−0.008	0.026	0.743	−0.432
Density	0.226	0.224	−0.266	0.893
V_p	0.948	−0.144	0.028	−0.009
V_s	0.688	−0.708	0.051	0.084
V_p/V_s	−0.091	0.941	−0.212	0.122
log(ε)	0.418	−0.122	0.870	0.137
E_d	0.807	−0.563	0.065	−0.061
v_d	−0.049	0.958	−0.024	0.230

4.1.1. Component 1: principal related variables: V_p [0.948]; Class2 [−0.885]; E_d [0.807] and V_s [0.688]

This component reveals a strong interaction between three ultrasonic parameters (velocity of the wave *P*, *S* and Young's modulus), with the percentage of small clasts in the sample (the petrographic parameter Class2). These relationships are inverse: the coefficient of the Class2 is negative, while V_p, V_s and E_d coefficients are positive. The inverse relationship of these relationships can be observed more clearly in the regression line trend of the scatter diagrams of these four parameters showed in Fig. 5.

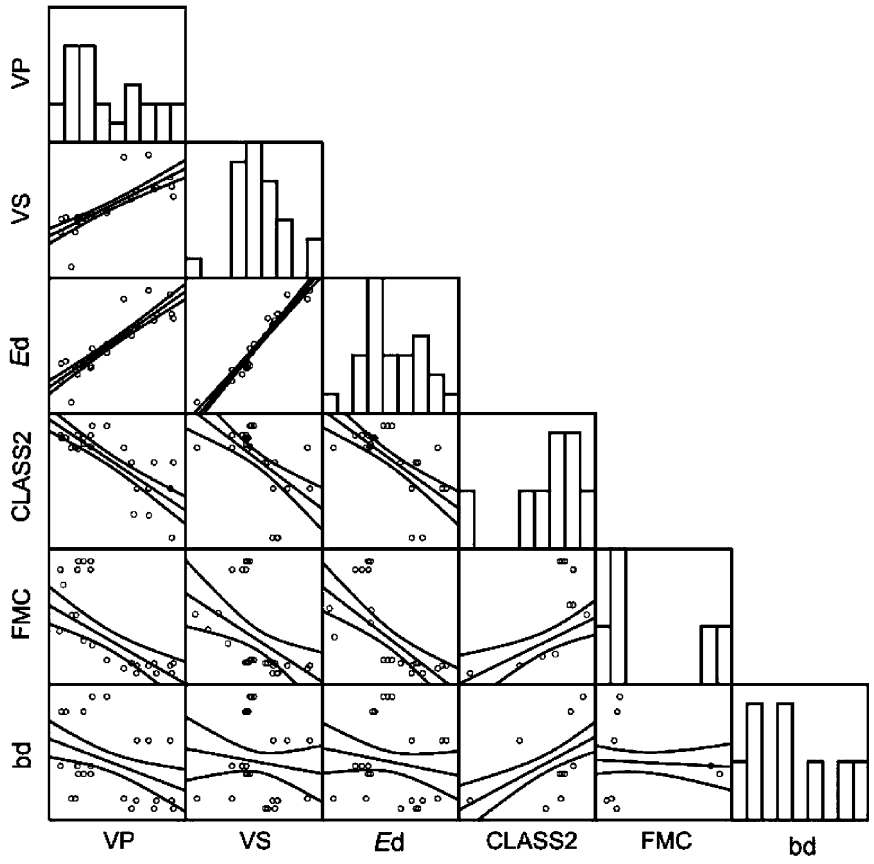

Fig. 5. Relationships between V_p, V_s, Young's modulus, Class2, FMC and *bd*. Each scatter diagram shows the regression line and the 50% confidence limits. These confidence limits show the interval in which a new data will be included with a 50% probability. The bar graphs of the diagonal show the frequency histograms of the corresponding variable.

According to these results, the greater the amount of small clasts, the lower the velocities and the E_d. This assertion can be explained by the fact that a higher content of small clasts in the sample is equivalent to a lower homogeneity, and a greater number of discontinuities. On the one hand, when a wave strikes in a discontinuity, it suffers scattering processes as well as a delay in its propagation. That explains the high connection between V_p, V_s and Class2. On the other hand, it is well known the fact that fractures and discontinuities generate an inelastic yielding in the mechanical behaviour of samples [33]. Therefore, it explains the relationship between Class2 and E_d.

In particular, the considerable high coefficient of FMC [−0.470], and the negative sign of both FMC and Class2 [−0.885] allow us to affirm that the high number of small clasts, the high fine-grained matrix content and, therefore, the high calcite content. The velocity of the ultrasonic waves in a dolomite medium is greater than in a calcite medium. So, the increase of small clasts, and the increase of calcite content, is directly related to the decrease of V_p and V_s.

4.1.2. Component 2: principal related variables: v_d [0.958]; V_p/V_s [0.941]; V_s [−0.708] and E_d [−0.563]

Component 2 shows some well-established relationships: (1) between Poisson's ratio and the V_p/V_s parameter, which is quantified by Eq. (2); (2) between shear wave velocity and elastic constants, suggested previously in component 1; and (3) between Young's modulus and Poisson's ratio.

These relationships show the well-established equations from the theory of elasticity and manifest the effectiveness of the principal component analysis to grouping of the different parameters.

4.1.3. Component 3: principal related variables: log(ε) [0.870]; bd [0.772]; α_{lim} [−0.758] and Class5 [0.743]

In this component, an interesting relationship is observed between the ultrasonic parameter log(ε) (logarithm of the energy of the registered waveform) and the three petrographic parameters: α_{lim}, *bd* and Class5.

One of the most interesting results obtained from this study is the connection showed between the parameter α_{lim} and log(ε). This relationship provides information about the sensitivity of waveform energy to determine the orientation of discontinuities in the sample. The opposite coefficient signs of the two parameters show that a greater number of clasts and discontinuities orientated between the worst ultrasonic propagation angles create intensive scattering processes and, therefore, a reduction in waveform energy. The inverse trend between both variables can be observed more clearly in Fig. 6, where the scatter

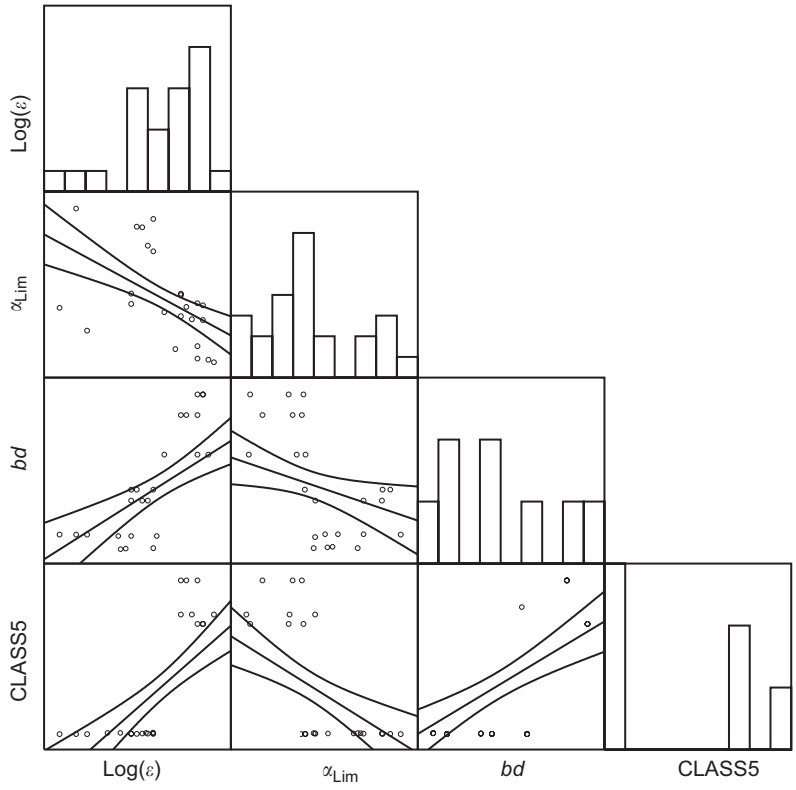

Fig. 6. Relationships between log(ε), α_{lim}, *bd* and Class5. Each scatter diagram shows the regression line and the 50% confidence limits. These confidence limits show the interval in which a new data will be included with a 50% probability. The bar graphs of the diagonal show the frequency histograms of the corresponding variable.

diagram is shown (as well as the scatter diagrams of the rest of parameters connected in this component).

On the other hand, it is also important to remark the high values which relate the ultrasonic parameter log(ε), and the petrographic parameters *bd* and Class5. All this coefficients have positive values, which reveal a direct relationship between all of them, as we can observe in the regression line trend of the scatter diagrams showed in Fig. 6. These connections indicate that the greatest waveform energies are associated with samples with both a high clast density and high large clast content. The previous assertion allows us to affirm that the samples with a high clast density and large clast content present a low number of discontinuities. According to wave propagation theory, when the number of discontinuities decrease, ultrasonic wave attenuation decreases and, consequently, the waveform energy increases. This explains the relationship observed between the waveform energy and both the clast density and clast content. As a conclusion, samples in which high waveform energy is registered, present higher rock fabric homogeneity (in terms of brecciation degree).

4.1.4. Component 4: principal related variables: density [0.893] and FMC [0.815]

A relationship between the fine-grained matrix content and the density of the sample is observed in the component 4. The high positive values of both coefficients indicate that the higher the fine-grained matrix content, the higher the density. This relationship could be contradictory due to the fact that the calcite density is lower than the dolomite density. Consequently, a sample with high fine-grained matrix content has a high calcite content, and theoretically, it should have a low density. However, according to the values shown in [33], calcite density is very similar to dolomite density ($\rho_{calcite} = 2.71\,g/cm^3$; $\rho_{dolomite} = 2.86\,g/cm^3$). Therefore, variations in density cannot be explained by simply taking into account the density of mineralogical components, as such features as, for example, the porosity associated to different textures (idiotopic or xenotopic) [34] is more influential on density value than the calcitic content of the sample.

4.2. Cluster analysis

Cluster analysis is a multivariate technique used to find homogeneous groups with respect to certain properties. For this reason, this tool has been used in order to study the similarities in the different samples studied. All of the petrographic parameters obtained via image analysis and the density of each sample were considered.

Fig. 7 shows the obtained results. Two different clusters can be seen in the samples used. These two groups correspond exactly to the two varieties considered in this study. This result is proof of the correct quantification of

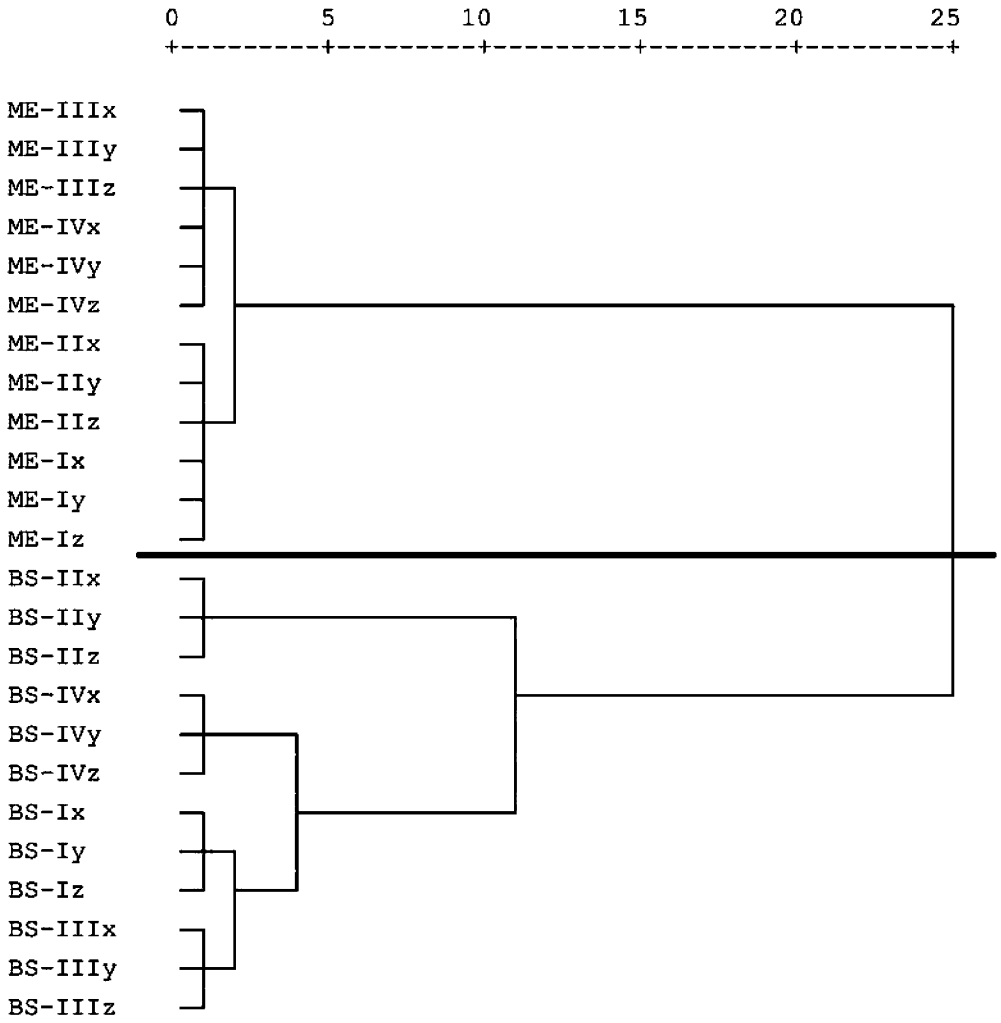

Fig. 7. Samples grouped according to their petrographic characteristics and their density via cluster analysis.

the petrography of these materials, as well as the discriminatory nature of the petrographic variables. Moreover, this result supports the fact that the conclusions obtained in the multivariate analysis are not only valid for one specific material, but for fractured carbonated rocks.

On the other hand, due to the fact that measurements of several petrographic and ultrasonic aspects depend on the direction considered, values in the three orthogonal axes of each sample have been considered in this analysis. Results shown that the three values for each sample are always in the same cluster. This fact shows the relatively low anisotropy of the samples studied between their axial directions. However, the BS variety is a more heterogeneous material than ME, due to the fact that the distances measured between the different clusters are larger.

5. Conclusion

In order to study the influence of the petrography of highly fractured rocks in the propagation of ultrasonic waves, different multivariate analysis techniques have been used (scatter diagrams, principal components and cluster analysis). To carry out this analysis, it was necessary to create a database containing all of the petrographic and ultrasonic parameters. Petrographic quantification was carried out via colour analysis of the mesoscopic images of the scanned sample. Due to the complex characteristics of the two different varieties of brecciated dolostones used as samples in this study, a new image analysis methodology was designed. The outcome of this methodology are several numeric petrographic parameters which quantify the most important characteristics of the samples studied in order to elaborate a database to be used in the multivariate analysis. On the other hand, an in-depth analysis of elastic wave propagation was carried out using ultrasonic signal digital analysis. The waveform has been quantified in detail by four ultrasonic parameters: compressive and shear wave velocities, velocity ratio and waveform energy. Elastic dynamic constants, Young's modulus and Poisson's ratio, were also calculated.

The most important results obtained from the multivariate analysis can be summarised in the following three points:

(a) Ultrasonic wave velocity and Young's modulus are controlled by both the number of discontinuities and the mineralogy (calcite content) of the sample. This is due to the fact that discontinuities and fractures generate scattering and delay in wave propagation, as well as an inelastic yielding in the sample. On the other hand, ultrasonic wave velocity in a dolomite medium is greater than in a calcite medium. Therefore, variations in the mineral content are directly related to variations in V_p and V_s.
(b) Waveform energy is a new sensitive parameter, which can assess the existence of predominant fracture sets or preferred orientations in the cracks. Waveform energy is not usually calculated in most ultrasonic studies. However, according to the results of this study, this is an extremely useful and highly sensitive ultrasonic parameter that can be used to assess the presence and orientation of fracture sets. This is due to the fact that fractures and discontinuities in the rock can cause important wave scattering processes and, therefore, increase ultrasonic wave attenuation and decrease waveform energy.
(c) Cluster analysis reveals two different clusters in the samples used. These two groups correspond exactly to the two varieties considered in this study. This result is interesting in that it provides proof of the correct quantification of the petrography of these materials, as well as the discriminatory nature of the petrographic variables. Moreover, this result supports the fact that the conclusions obtained in the multivariate analysis are not only valid for one specific material, but for all fractured carbonated rocks.

According to the results obtained in this study, ultrasounds are an extremely powerful tool for evaluating the mechanical characteristics of highly fractured rocks. With this non-destructive technique, it is possible to assess the elastic behaviour of rocks, as well as the degree of fracturing, preferred orientation of the cracks, etc. Knowledge about these aspects is particularly important as they control many of the processes involved in stone decay and the mechanical changes in the rock. However, further research into the proposed methodology is necessary in order to corroborate the relationships obtained, as well as to define more precise correlations between both ultrasonic and petrographic variables. This could be done by increasing the number of tested samples and analysing new types of fractured materials.

Acknowledgements

This study was financed by the Spanish Ministry of Education and Science (Spain): Research Project MAT 2003-01823; and the Generalitat Valenciana (Spain): Project GV04B-630. A pre-doctoral research fellowship was awarded to J. Martínez-Martínez by the Higher Council of Scientific Research (CSIC, Spain). The authors are grateful to Esteve & Máñez S.A. for supplying the materials used. The authors would like to thank the anonymous reviewers for their many incisive comments and criticisms in revising this article.

References

[1] Akesson U, Stigh J, Lindqvist JE, Göransson M. The influence of foliation on the fragility of granitic rocks, image analysis and quantitative microscopy. Eng Geol 2003;68:275–88.
[2] Ersoy A, Waller MD. Textural characterisation of rocks. Eng Geol 1995;39:123–36.
[3] Hatzor YH, Palchik V. The influence of grain size and porosity on crack initiation stress and critical flaw length in dolomites. Int J Rock Mech Min Sci 1997;34:805–16.
[4] Hatzor YH, Zur A, Mimran Y. Microstructure effects on microcracking and brittle failure of dolomites. Tectonophysics 1997;281:141–61.
[5] Prikryl R. Some microstructural aspects of strength variation in rocks. Int J Rock Mech Min Sci 2001;38:671–82.
[6] Palchik V, Hatzor YH. Crack damage stress as a composite function of porosity and elastic matrix stiffness in dolomites and limestones. Eng Geol 2002;63:233–45.
[7] Song I, Elphick SC, Odling N, Main IG, Ngwenya BT. Hydro-mechanical behaviour of fine-grained calcilutite and fault gouge from the Aigion Fault Zone, Greece. C R Geosci 2004;336:445–54.
[8] Tham LG, Li L, Tsui Y, Lee PKK. A replica method for observing microcracks on rock surfaces. Int J Rock Mech Min Sci 2003;40:785–94.
[9] Volland S, Kruhl J. Anisotropy quantification: the application of fractal geometry methods on tectonic fracture patterns of a Hercynian fault zone in NW Sardinia. J Struct Geol 2004;26:1499–510.
[10] Sousa LMO, Suárez del Río LM, Calleja L, Ruiz de Argandoña VG, Rodríguez Rey A. Influence of microfractures and porosity on the physico-mechanical properties and weathering of ornamental granites. Eng Geol 2005;77:153–68.
[11] Saotome A, Yoshinaka R, Osada M, Sugiyama H. Constituent material properties and clast-size distribution of volcanic breccia. Eng Geol 2002;64:1–17.
[12] Boadu FK. Fractured rock mass characterization parameters and seismic properties: analytical studies. J Appl Geophys 1997;36:1–19.
[13] Valdeon L, Freitas MH, King MS. Assessment of the quality of building stones using signal processing procedures. Q J Eng Geol 1997;29:299–308.
[14] Tugrul A, Zarif IH. Correlation of mineralogical and textural characteristics with engineering properties of selected granitic rocks from Turkey. Eng Geol 1999;51:303–17.
[15] Donald JA, Butt SD, Iakovlev S. Adaptation of a triaxial cell for ultrasonic *P*-wave attenuation, velocity and acoustic emission measurements. Int J Rock Mech Min Sci 2004;41:1001–11.
[16] Beard MD, Lowe MJS. Non-destructive testing of rock bolts using guided ultrasonic waves. Int J Rock Mech Min Sci 2003;40:527–36.
[17] Benson PM, Meredith PG, Platzman ES, White RE. Pore fabric shape anisotropy in porous sandstones and its relation to elastic wave velocity and permeability anisotropy under hydrostatic pressure. Int J Rock Mech Min Sci 2005;42:890–9.
[18] Donald JA, Butt SD. Experimental technique for measuring phase velocities during triaxial compression tests. Int J Rock Mech Min Sci 2005;42:307–14.

[19] Meglis IL, Chow T, Martin CD, Young RP. Assessing in situ microcrack damage using ultrasonic velocity tomography. Int J Rock Mech Min Sci 2005;42:25–34.
[20] Benavente D, Martínez-Martínez J, Jáuregui P, Rodríguez MA, García del Cura MA. Assessment of the strength of building rocks using signal processing procedures. Constr Build Mater 2006;20(8):562–8.
[21] Reinhardt HW, Grosse CU. Continuous monitoring of setting and hardening of mortar and concrete. Constr Build Mater 2004;18: 145–54.
[22] Zhao J, Zhao XB, Cai JG. A further study of *P*-wave attenuation across parallel fractures with linear deformational behaviour. Int J Rock Mech Min Sci 2006;43:776–88.
[23] Song I, Suh M, Woo Y, Hao T. Determination of the elastic modulus set of foliated rocks from ultrasonic velocity measurements. Eng Geol 2004;72:293–308.
[24] Martínez-Martínez J, Benavente D, Rodríguez MA, García del Cura MA. Ensayos destructivos y no destructivos (ultrasonidos) en la determinación de calidad de rocas ornamentales: aplicación a dolomías brechoides. Geogaceta 2004;35:107–10.
[25] Martínez-Martínez J, Benavente D, García del Cura MA. Petrographic quantification of fractured rocks by image analysis. Application to the interpretation of elastic wave velocities. Eng Geol 2007;90: 41–54.
[26] Sardini P, Sammartino S, Tévissen E. An image analysis contribution to the study of transport properties of low-permeability crystalline rocks. Comp Geosci 2001;27:1051–9.
[27] Andriani GF, Walsh N. Physical properties and textural parameters of calcarenitic rocks: qualitative and quantitative evaluations. Eng Geol 2002;67:5–15.
[28] Cueto N, Benavente D, García del Cura MA. Influencia de la anisotropía en las propiedades hídricas de rocas. Estudio de rocas dolomíticas brechoides de la Cordillera Bética (España). Geogaceta 2006;40:315–8.
[29] Arau H. ABC de la acústica arquitectónica. Barcelona: CEAC Eds; 1999.
[30] Durá AD. Temas de acústica. Alicante: Publicaciones de la Universidad de Alicante; 2005.
[31] Jaeger JC, Cook NGW, Zimmerman RW. Fundamentals of rock mechanics. 4th ed. Oxford: Blackwell; 2007.
[32] Davis JC. Statistics and data analysis in geology. New York: Wiley; 1973.
[33] Schön JH. Physical properties of rocks: fundamentals and principles of petrophysics. New York: Pergamon; 1996.
[34] Hatzor YH, Zur A, Mimran Y. Microstructure effects on microcracking and brittle failure of dolomites. Tectonophysics 1997;281: 141–61.